AIAA JOURNAL
Vol. 39, No. 6, June 2001

Engineering Application of Oxygen Laser-Induced Fluorescence Temperature Measurements in Aerodynamic Flows

Ismail Ceyhan* and Alan H. Epstein†
Massachusetts Institute of Technology, Cambridge, Massachusetts 02139

Oxygen laser-induced fluorescence was studied experimentally to quantify significant error and uncertainty sources and to evaluate the technique feasibility for gas temperature measurements in the 1–6-atm, 300–500-K regime. The dominant uncertainty source is quantum noise. For low-speed flows, the dominant error source is nonlinear process errors originating from oxygen ion fluorescence and saturation. For flows where the pressure is unknown or variable, collisional quenching may introduce an additional error up to 3 K/atm. For high-speed flows above 300 K, the dominant error source is the slow vibrational relaxation time of oxygen molecules. The optimum experimental conditions are determined by budgeting the allowable temperature inaccuracy to various uncertainty and error sources. In general, the nonlinear process errors limit the laser fluence that may be used, and the quantum noise determines the minimum number of laser shots per measurement.

Nomenclature

E	=	laser fluence, J/cm^2
M	=	Mach number
N	=	number of laser shots per measurement
P	=	pressure (total), atm
P_{O_2}	=	partial pressure of oxygen, atm
R	=	temperature diagnostic ratio (TDR)
S_D	=	denominator signal for TDR, counts
S_N	=	numerator signal for TDR, counts
T	=	temperature, K
V	=	measurement volume, mm^3
v'	=	vibrational level of the upper electronic state
v''	=	vibrational level of the lower electronic state
W_2^C	=	collisional quenching rate of the upper electronic state, s^{-1}
x	=	distance from shock, cm
η_c	=	collection efficiency
σ_T	=	temperature uncertainty due to quantum noise, K
τ_v	=	vibrational relaxation time, s
Ω	=	collection solid angle, sr

Superscript

ref	=	reference conditions for Fig. 5

Introduction

THE objective of the current study is to evaluate the feasibility of oxygen laser-induced fluorescence (LIF) for gas temperature measurements in aerodynamic flows by quantifying the significant error and uncertainty sources. Future investigators may use the information developed in this study to design temperature measurement experiments.

One potential aerodynamic application for the oxygen LIF technique is gas temperature measurements in turbomachinery. Intrarotor temperature measurements in turbines may be used to study heat transfer to turbine blades. Interstage temperature measurements may also be taken in compressors to calculate stage efficiencies accurately. Finally, intrarotor temperature measurements may be combined with optical velocity measurements, for example, laser Doppler anemometry (LDA) or particle image velocimetry (PIV), to calculate the Mach number field that characterizes the intrarotor flowfield.

Oxygen LIF technique has several advantages for aerodynamic applications. Limited only by the 20-ns laser pulse duration, its temporal resolution is much better than the blade passing period in turbomachinery. The technique requires no seeding or cleanup because it uses the oxygen molecules present in ambient air. The technique provides an inherent wavelength shift so that the reflected laser light does not obscure the temperature-sensitive signals. Finally, the technique can be implemented using commercially available equipment.

The oxygen LIF technique was first proposed by Massey and Lemon in 1984 shortly after the development of the first excimer laser.[1] In 1986, Lee and Hanson developed a spectral model for calculating the temperature dependence of LIF signals.[2] Additional theoretical studies were published by Laufer et al. in 1988 (Ref. 3), Miles et al. in 1988 (Ref. 4), and Smith et al. in 1993 (Ref. 5). Between 1986 and 1996, qualitative results were obtained on high-temperature methane–air flames,[6] supersonic freejets,[7] and hypersonic wind-tunnel flows.[8,9] Of these studies, Refs. 1, 4, 5, 7, and 8 examine an ArF laser operating in narrowband mode, whereas Refs. 2, 3, 6, and 9 look at the laser operating in broadband mode.

Previous studies have claimed, but have not demonstrated, that less than 1-K temperature accuracy is feasible. This study experimentally quantifies the constraints on accuracy and precision.

Oxygen LIF Temperature Measurement Theory

Oxygen LIF technique measures gas temperature by probing the distribution of oxygen molecules among quantum states of the ground electronic state. Because the distribution of molecules among quantum states is a strong function of temperature, the LIF signal magnitude also depends on temperature. The technique uses this temperature dependence to determine the gas temperature.

A broadband ArF excimer laser is used to excite transitions in the $B^3\Sigma_u^- \leftarrow X^3\Sigma_g^-$ Schumann–Runge band. Only those transitions that are overlapped by the ArF spectrum at 193 nm are excited. Each excited molecule absorbs a single photon from the incident laser light. The excited transitions originate from the $v''=0$, 1, and 2 vibrational levels of the ground electronic state and fill, respectively, the $v'=4$, 7, and 10 vibrational levels of the upper electronic state.

LIF emission is generated as some of the excited molecules spontaneously decay back to the ground electronic state. Each decaying molecule emits a single photon. The wavelength of the emitted photon is related to the energy separation between the upper and lower states of the fluorescence transition.

The LIF signal magnitude is a strong function of temperature. Only those molecules that are in the quantum states accessed by the ArF laser are excited to the upper electronic state and may later fluoresce. Therefore, the LIF signal magnitude is proportional to the number of molecules in the accessed quantum states. The

Received 24 January 2000, revision received 15 November 2000; accepted for publication 6 January 2001.

*Research Assistant, Gas Turbine Laboratory, 77 Massachusetts Avenue, Room 31-264; ceyhan@stanfordalumni.org. Member AIAA.

†Professor, Gas Turbine Laboratory, 77 Massachusetts Avenue, Room 31-264; epstein@mit.edu. Fellow AIAA.

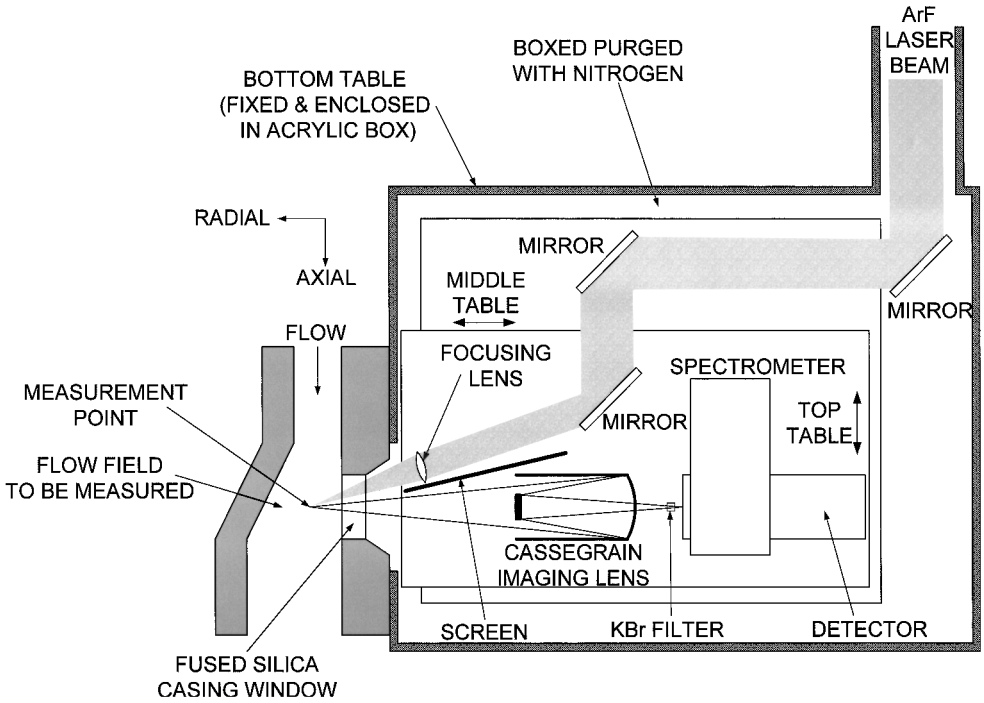

Fig. 1 Experimental apparatus schematic.

distribution of molecules among quantum states is an exponential function of temperature as given by the Boltzmann distribution. The LIF temperature measurement technique uses this temperature dependence of the LIF signal to determine the gas temperature.

More details about the LIF temperature measurement theory may be found by Lee and Hanson[2] and by Ceyhan.[10]

Experimental Apparatus

The experimental apparatus was designed for intrarotor temperature measurement in turbomachinery rigs. Figure 1 presents a schematic of the experimetal apparatus. An oblique-scatter arrangement was chosen because of the limited access to the flowfield in turbomachinery.

A Lambda–Physik EMG160MSC excimer laser operating in broadband mode at 193 nm with an ArF gas fill was used. The laser was capable of operating in either narrowband or broadband mode; however, all data presented in this paper were acquired with the laser in broadband mode. A cryogenic purification system was implemented to increase the life of the gas fill.

The laser beam was steered to the measurement point using six turning mirrors. A fused silica, plano-convex lens was used to focus the laser beam through a fused silica casing window to the measurement point. The focal length of the lens was 127 mm at 587 nm (104.3 mm at 193 nm).

The LIF signals were collected using a cassegrain telescope lens (Lyman Alpha I manufactured by NYE Optical Co.) operating at a paraxial magnification of 0.78. The collected light was dispersed using an Acton Research SpectraPro 275 spectrometer. A potassium bromide (KBr) disk was placed at the entrance of the spectrometer to filter contaminating signals due to reflection from the casing window and internal surfaces, as well as the signals due to Rayleigh scattering. The spectrometer slit width was 140 μm, and a 1200 mm^{-1} grating centered at 234 nm was used. The resulting range and resolution were 200–270 nm and 0.68 nm (full width at half maximum), respectively.

The dispersed signals were recorded using a Princeton Instruments IDPA-1024 intensified photodiode array. The detector contained 1024 diodes, each of which was 25 μm wide and 25 mm high. To minimize dark charge, the detector was thermoelectrically cooled to -20°C. Signals from multiple laser shots were accumulated on the diodes, and the overall counts were read, digitized, and recorded using a personal computer.

To eliminate loss of signal due to absorption by oxygen molecules in the ambient atmosphere, the entire apparatus (including laser optics) was enclosed in an acrylic box, which was purged with nitrogen. A three-table positioning system was designed so that the measurement point could be relocated along two axes without having to realign the optics. (The position along the third axis could be chosen by adjusting the delay between each laser pulse and blade passage.)

Data for calibration and error analysis were obtained with the measurement apparatus located in front of a heated air test cell. The test cell temperature and pressure were regulated and measured. The temperature measurement was performed with a thermocouple probe, which was retracted from the measurement point just before the LIF measurement process was initiated. The test cell was designed for 300–600-K temperature and 1.3–6.5-atm pressure ranges.

Although the experimental apparatus was designed for temperature measurements in experimental turbomachinery rigs, the results discussed are applicable to the oxygen LIF temperature measurement technique in general.

Data Reduction Procedure

Spectral normalization was determined to be the most accurate method for calculating gas temperature from the recorded oxygen LIF spectrum. The spectral normalization method accounts for the linear dependence of the fluorescence signals on laser fluence, measurement volume, gas pressure, collection solid angle, and collection efficiency. Rayleigh, Raman, and two-line normalizations were either not feasible or less accurate than spectral normalization for the 300–550-K temperature range of interest in this study.

In addition to temperature, the oxygen LIF emission depends on laser fluence (defined as the laser beam energy divided by the beam area), measurement volume, gas pressure, collection solid angle, and collection efficiency. Theoretically, the LIF signal dependencies on these extraneous parameters are linear. It is necessary to account for these dependencies to extract temperature information from the LIF signals.

Over the 300–550-K temperature range of interest, the most accurate method was determined to be spectral normalization. In spectral normalization, temperature-insensitive LIF signals are used to normalize temperature-sensitive LIF signals. The temperature-sensitive signals originate from the molecules excited from the $v'' = 1$ and 2 vibrational levels. The relatively temperature-insensitive signals

originate from the molecules excited from the $v''=0$ vibrational level.

Temperature-sensitive and temperature-insensitive signals are spectrally separated because the molecules excited from different vibrational levels exhibit different fluorescence signatures. For example, the temperature-sensitive $v''=1$ and 2 signals are strongest around 220 and 207 nm, respectively. The temperature-insensitive $v''=0$ signals are strongest between 232–234 and 240–242 nm. Consequently, the LIF spectrum strength shifts toward the shorter wavelengths as temperature increases both within each peak region and overall (Fig. 2). In Fig. 2, the feature at 202.5 nm is the nitrogen Raman signal, which is partially obscured by the KBr spectral filter.

In a normalization scheme, the temperature is obtained from a temperature diagnostic ratio (TDR):

$$R(T) = S_N / S_D \tag{1}$$

For quantum-noise-limited measurements, the resulting temperature uncertainty is given by the following expression:

$$\sigma_T \sim \frac{R/\sqrt{S_N}}{|\mathrm{d}R/\mathrm{d}T|}(1+R)^{\frac{1}{2}} \tag{2}$$

Temperature-sensitive signals are assigned to the numerator to maximize TDR sensitivity. In addition, the magnitudes of the numerator and denominator are kept of equal order, that is, $R \sim 1$. Otherwise, the temperature uncertainty would be dominated by the weaker signal.

In this study, the data reduction proceeded as follows.

1) A background was subtracted from the oxygen LIF spectrum. The background was recorded under the same experimental conditions as the oxygen LIF spectrum except that the laser was not firing. The background primarily represents the dark counts collected on the detector diodes due to random thermal processes.

2) The remaining oxygen LIF signal was divided into 13 regions. The regions are shown in Fig. 3, where the total signal in each region is calculated by summing the counts from appropriate diodes. The regional signals are assigned to the numerator or denominator of the temperature diagnostic ratio based on their temperature sensitivity. Their boundaries are listed in Table 1. Table 1 shows initial (v') and final (v'') vibrational levels for the emission transition: $v'=4$ levels are filled by absorption transitions originating from the $v''=0$ level, $v'=7$ levels are filled from the $v''=1$ level, and $v'=10$ levels are filled from the $v''=2$ level. Only the dominant transitions in each region are listed.

3) The signal in each region was calculated by summing the count readings from the member diodes.

4) The numerator and denominator were computed by summing the appropriate regional signals. Table 1 indicates whether a regional signal belongs to the numerator or denominator.

5) TDR was computed using Eq. (1).

6) Temperature was then determined from a $T(R)$ function. The $T(R)$ function was calibrated against thermocouples in a calibration cell. Figure 4 shows the $T(R)$ calibration function used in this study. The temperature sensitivity is highest between 400 and 525 K.

Other normalization methods were found to be either not feasible or less accurate than spectral normalization. Normalization by the oxygen Raman signals is not feasible because the Rayleigh signals are obscured by the KBr spectral filter, which is necessary to eliminate reflected laser light. The fundamental oxygen Raman signal at 199.4 nm is completely obscured by the spectral filter, and the second-order oxygen Raman signal at 205.7 nm is obscured at higher temperatures by the underlying $v''=2$ LIF signals. In addition, normalization by the nitrogen Raman signal was determined to be less accurate than spectral normalization, especially at higher temperatures. The KBr filter transmits only 36% of the nitrogen Raman signal at 202.5 nm, and the transmitted nitrogen Raman signal ranges between 10% (at 300 K) and 1.3% (at 500 K) of the oxygen LIF signal.

Curve fitting using nonlinear optimization techniques was also found to be less accurate than spectral normalization. Curve fitting

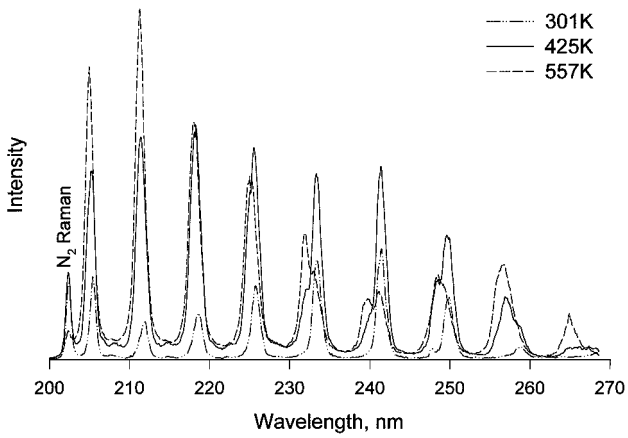

Fig. 2 Oxygen LIF spectra recorded at 301, 425, and 557 K.

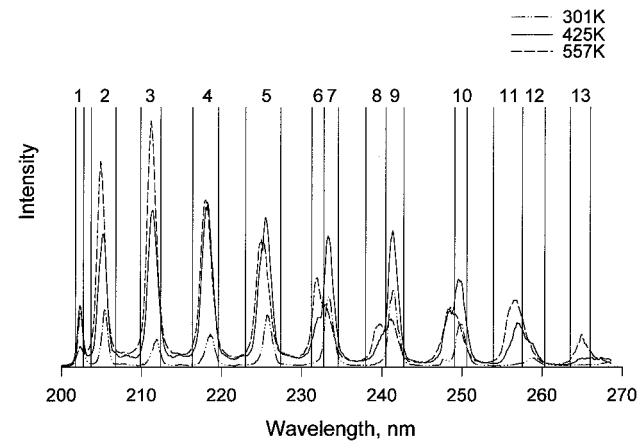

Fig. 3 Oxygen LIF spectra divided into 13 regions for data reduction.

Table 1 Regional signal boundaries and assignments

Region	Wavelength range, nm	Number of channels[a]	Assignment	Main emission features (v', v'')
1	201.76–202.77	14	Denominator	N_2 Raman
2	203.70–206.08	33	Numerator	(4,2) (7,3) (10,4)
3	209.89–212.41	35	Numerator	(7,4) (10,5)
4	216.36–219.60	45	Numerator	(7,5)
5	222.98–227.37	61	Numerator	(7,6)
6	231.25–232.76	21	Numerator	(7,7) (10,8)
7	232.76–234.56	25	Denominator	(4,6) (10,8)
8	237.97–240.46	35	Numerator	(10,9)
9	240.46–242.69	31	Denominator	(4,7)
10	249.09–250.60	21	Denominator	(4,8) (7,9)
11	253.91–257.51	50	Numerator	(7,10) (10,11)
12	257.51–260.31	39	Denominator	(4,9) (7,10) (10,11)
13	263.48–265.99	35	Denominator	(4,10) (10,12)

[a]There is a 1024-channel diode array located at the 25-mm-wide focal plane of 275-mm-focal-length spectrometer with 1200 mm^{-1} grating centered at 234 nm.

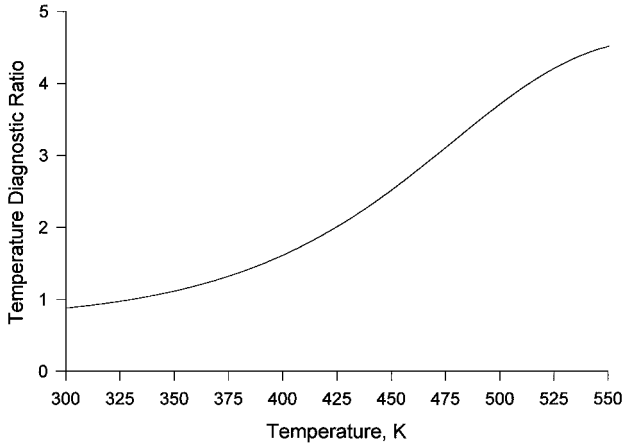

Fig. 4 Temperature diagnostic ratio calibration curve.

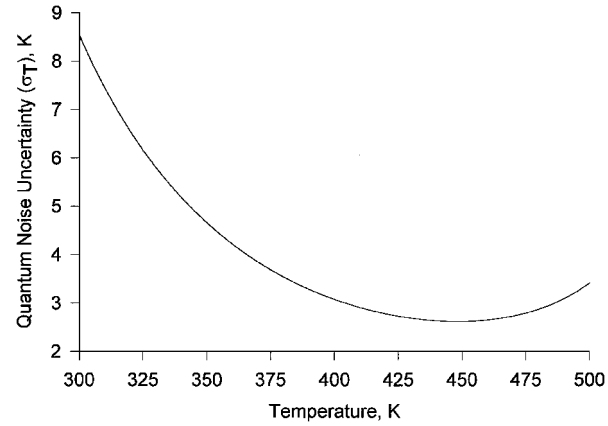

Fig. 5 Single-shot quantum-noise-limited temperature measurement uncertainty as a function of temperature at the indicated reference conditions.

uses the analytical signal shape information to reduce the measurement uncertainty.[11] However, the oxygen LIF signals consist of many closely spaced peaks that are not resolved under the measurement conditions. It is not possible to describe the composite signal shape with analytical functions.

Error and Uncertainty Sources

For low-speed measurements, the dominant error source is nonlinear processes. Collisional quenching may also be significant. For high-speed measurements, the dominant error source is vibrational relaxation. The uncertainty and error sources are discussed individually next.

Quantum Noise

For both low-speed and high-speed measurements, the dominant uncertainty source is quantum noise. Measurement uncertainty due to quantum noise may be reduced by increasing laser fluence, measurement volume, collection solid angle, and collection efficiency, as well as by integrating LIF signals from multiple laser shots.

Quantum noise is the statistical variation introduced to the radiative signals due to the discrete (quantum) nature of light. Any interaction between light and matter is a source of quantum noise. In the oxygen LIF technique, such light–matter interactions include the production of laser radiation, the absorption of laser light by oxygen molecules, the fluorescence by oxygen molecules, and the detection of LIF signals.

Quantum noise is governed by the Poisson distribution.[12] For 10 or more counts, the Poisson distribution approaches the normal error (Gaussian) distribution.[13] The standard deviation of the quantum noise distribution is proportional to the square root of the signal level.

Figure 5 shows the single-shot quantum uncertainty for the particular apparatus used in this study. Quantum uncertainty may be reduced by increasing laser fluence, measurement volume, collection solid angle, and collection efficiency. In addition, quantum uncertainty may be reduced by integrating LIF signals resulting from multiple laser shots. The following equation may be used to scale uncertainty values obtained from Fig. 5 to other experimental conditions:

$$\sigma_T = \sigma_T^{\text{ref}} \sqrt{\left(\frac{E^{\text{ref}}}{E}\right)\left(\frac{P_{O_2}^{\text{ref}}}{P_{O_2}}\right)\left(\frac{V^{\text{ref}}}{V}\right)\left(\frac{\Omega^{\text{ref}}}{\Omega}\right)\left(\frac{\eta_c^{\text{ref}}}{\eta_c}\right)\left(\frac{N^{\text{ref}}}{N}\right)} \tag{3}$$

For Fig. 5, $E^{\text{ref}} = 10\,\text{J/cm}^2$, $P_{O_2}^{\text{ref}} = 1\,\text{atm}$, $V^{\text{ref}} = 1\,\text{mm}^3$, $\Omega^{\text{ref}} = 0.1\,\text{sr}$, $\eta_c^{\text{ref}} = 0.01$, and $N^{\text{ref}} = 1$ shot. With the normal distribution, 68.3% of the temperature readings may be expected to fall within $\pm\sigma_T$ of the mean value.

If the LIF signal levels are too low, the uncertainty will be dominated by the detector noise. Detector noise originates from readout uncertainty as well as thermal charges accumulating on the diodes. Significance of detector noise may be lowered by on-detector integration of LIF signals from multiple laser shots before readout. If an intensified detector is used, increasing the intensifier gain will also reduce the contribution of detector noise to measurement uncertainty.

Nonlinear Process Errors

For low-speed flow measurements, the nonlinear processes are the dominant error source, namely, oxygen ion (O_2^+) fluorescence and saturation. Nonlinear processes introduce laser fluence dependencies to the TDR. The laser fluence needs to be limited to reduce the resulting error in the measured temperature.

Oxygen ion LIF signals exhibit a cubic dependence on laser fluence and do not depend on temperature (except through density). Oxygen ion LIF signals are concentrated in the same spectral regions as the temperature-sensitive oxygen LIF signals. Consequently, oxygen ion LIF process robs the TDR of its temperature sensitivity at lower temperatures. At higher temperatures, the oxygen ion LIF signals are weaker compared to the oxygen LIF signals, and oxygen ion LIF is of lesser importance as an error source.

Saturation results from the ArF laser depleting the ground states of the absorption transitions. In general, $v'' = 1$ and 2 transitions are more sensitive to saturation due to their higher transition probabilities. Consequently, saturation results in a fluence-dependent reduction in the temperature-sensitive LIF signals. The saturation error increases with increasing temperature as $v'' = 1$ and 2 transitions become stronger.

Temperature error due to nonlinear phenomena is shown in Fig. 6 as a function of temperature and laser fluence. Figure 6 is based on experimental data obtained at nine different temperatures between 297 and 507 K. Oxygen ion LIF is the dominant error source for temperatures less than 430–460 K. Saturation is the dominant error source for temperatures above 430–460 K. Around 430–460 K, the two error sources balance. The upper and lower laser fluence limits for the experimental data are also shown (dashed lines).

The laser fluence at which nonlinear process errors become significant is determined by the accuracy required and the experimental conditions. The ideal laser fluence is determined by balancing the uncertainty and error sources. An example is provided later.

Collisional Quenching

Collisional quenching may be a secondary but significant error source. Collisional quenching results from the excited molecules being moved out of the upper electronic state before fluorescencing as a result of collisions with other molecules. This quenching effect introduces pressure dependency to the TDR and the measured temperature. Previous studies had neglected collisional quenching as an error source based on the argument that the predissociation rate was significantly higher than the collisional quenching rate.[1,2,8]

This study indicates that the pressure-dependent temperature error introduced through collisional quenching may be as large as 3 K/atm. Figure 7 shows the collisional quenching error as a function

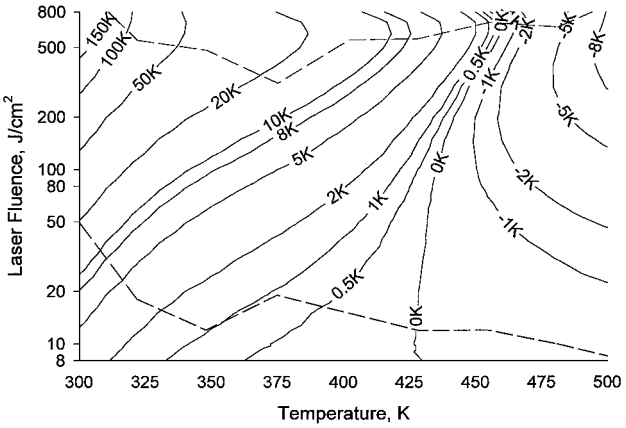

Fig. 6 Experimentally determined temperature measurement error due to nonlinear phenomena.

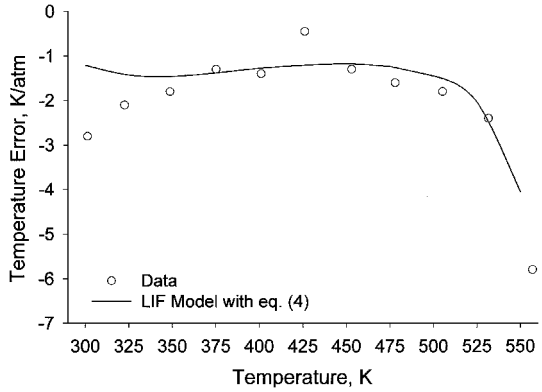

Fig. 7 Temperature measurement error due to collisional quenching.

of temperature. Collisional quenching error is significant for flows where the pressure is unknown, variable (e.g., compressible flows), or different from the calibration pressure. For measurements where the pressure is known, collisional quenching error may be avoided by calibrating the TDR at the flow pressure.

The data obtained during this study indicate that the following correlation may be used for collisional quenching rate of oxygen molecules in spectroscopic models:

$$W_2^C = (5.3 \times 10^9\ \mathrm{s}^{-1})(300\ \mathrm{K}/T)^{0.7}\left(P_{O_2}/0.2\ \mathrm{atm}\right) \qquad (4)$$

This correlation was derived from an empirical model given by Cann et al.[14] for pressure broadening linewidths of oxygen absorption transitions. The data suggest that only oxygen–oxygen collisions are effective in quenching the upper electronic state.

The data used for collisional quenching study were obtained in the heated air test cell with regulated pressure and temperature. The test cell temperature was separately measured using a thermocouple probe. Data were taken with the test cell pressure set at 1.4, 2.7, 3.8, 4.8, and 6.1 atm. At each pressure, LIF spectra were obtained at 11 temperatures between 301 and 557 K. The TDR was computed for each temperature–pressure pair and plotted on Fig. 7. The results were then compared to the two collisions rate models found in the literature.[4,14]

Vibrational Relaxation

For high-speed flow measurements, the dominant error source is the slow vibrational relaxation rate for oxygen molecules. Above 300 K, this slow vibrational relaxation rate results in the LIF-measured temperature deviating from the true gas temperature of the flow.

Above 300 K, the LIF process measures the vibrational temperature that characterizes the molecule distribution among vibrational levels. However, the thermodynamic properties of the flow are governed by the rotational temperature that characterizes the molecule distribution among rotational levels. The LIF technique measures vibrational temperature because its temperature sensitivity originates from the $v''=1$ and 2 upper vibrational levels being filled. Although the population of the upper vibrational levels are small, their contributions to the total LIF signal are large due to their large transition probabilities. For example, at 425 K, the $v''=1$ and 2 vibrational levels, respectively, account for only 0.5 and 0.002% of the total number of molecules, but 51 and 13% of the total LIF signal.

If the flow undergoes a temperature change, both the vibrational and the rotational distributions must adjust, that is, relax, to the new temperature. Temperature changes in flows may originate from heat transfer or compressibility effects, for example, supersonic shocks. The rotational redistribution occurs much faster than the vibrational relaxation rate (within several molecular collisions). As a result, the LIF-measured temperature is not an accurate indicator of the true gas temperature during the period of vibrational relaxation.

The vibrational relaxation time for oxygen molecules may be estimated using the following correlation developed from the data given by Billing and Kolesnick[15]:

$$\tau_v = (15\ \mathrm{ms\ atm}/P)(300\ \mathrm{K}/T)^{4.8} \qquad (5)$$

After one vibrational relaxation time period, approximately 63% of the molecules will have been redistributed. It is necessary to wait five periods until less than 1% of the molecules remain to be redistributed.

For the LIF temperature measurement to be useful, the distance covered by the molecules during vibrational relaxation must be small compared to the spatial resolution requirement. The spatial resolution capability of the LIF technique in air is shown in Fig. 8 as a function of temperature. Figure 8 shows that the spatial resolution capability is limited by the vibrational relaxation rate of oxygen molecules. The minimum spatial resolution capability is taken as five times the distance covered by the flow over a characteristic relaxation time period.

The vibrational relaxation error source can be illustrated by considering the example shown in Fig. 9. Here, a supersonic flow undergoes a normal shock located at $x=0$. Upstream of the shock, $M=1.500$, $P=2.44$ atm, and $T=379$ K. Downstream of the shock, $M=0.701$, $P=6.00$ atm, and $T=500$ K (The flow conditions were chosen to yield the fastest vibrational relaxation time downstream of the shock within the temperature and pressure ranges of interest.) The flow speed downstream of the shock is 314 m/s, and the vibrational relaxation time is 0.22 ms. The flow covers 6.8 cm over one vibrational relaxation time period.

Just downstream of the shock, the LIF temperature measures the vibrational temperature, which is 379 K (the static temperature upstream of the shock). The error between LIF-measured and true temperatures is 121 K. After 6.8 cm (one vibrational relaxation time period), the error is reduced to 44 K (37% of the original error). It takes the flow 33 cm, or five vibrational relaxation time periods, before the error is reduced to less than 1 K. Consequently, the LIF

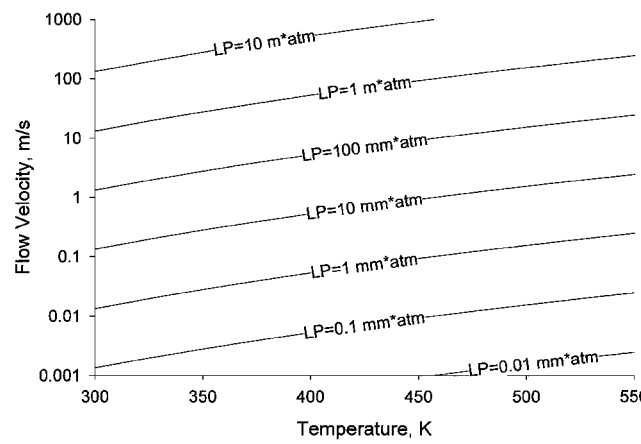

Fig. 8 Spatial resolution capability of the LIF technique as a function of temperature and flow speed.

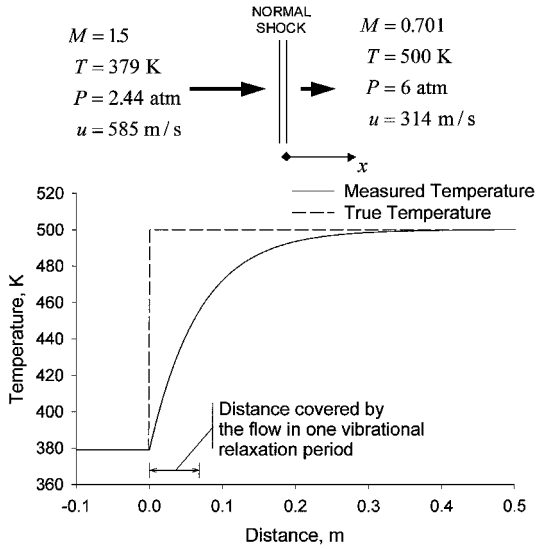

Fig. 9 Temperature error due to vibrational relaxation downstream of a normal shock.

technique cannot be used if the spatial resolution requirement is less than about 33 cm.

Vibrational relaxation error originates from flow speed rather than compressibility effects. Vibrational relaxation error will be significant unless the flow speed times the vibrational relaxation time is small compared to the spatial resolution requirement. Although compressible flows are typical examples of high-speed flows, vibrational relaxation may be a significant error source even when compressibility effects are negligible.

Above 300 K, the only conceptual technique known to the authors for avoiding the vibrational relaxation problem is to probe the rotational distribution of the $v''=0$ vibrational level. This may be accomplished in two ways.

1) A narrowband laser may be used to excite a $v''=0$ transition isolated from any $v''=1$ and 2 transitions. Only two transitions, namely, P(15) and P(19), satisfy this requirement. To avoid contamination by the $v''=1$ and 2 signals, the laser emission will have to remain perfectly narrowband from calibration until the measurements are completed. Also, only the nitrogen Raman signal is available to normalize the LIF signals.

2) An isolated emission line originating from the $v'=4$ level (which is filled by molecules excited from the $v''=0$ level) may be measured. However, there are no isolated $v'=4$ emission transitions within the 200–270 nm band for which the experimental apparatus was designed.

Below 300 K, vibrational relaxation does not introduce a temperature error because all LIF signals originate from the $v''=0$ level.

If only the rotational temperatures are probed, the achieavable temperature precision decreases due to several factors. First, the number of molecules being excited is reduced because only a single rotational level is being probed. Second, because of the lower energy associated with the $v''=0$ vibrational level, the rotational level being probed is mostly populated and its temperature sensitivity is low. Also, the signals must be normalized by the nitrogen Raman peak (the only uncontaminated signal that is temperature insensitive, except through density), whose strength decreases with increasing temperature (due to decreasing density). Finally, the laser fluence is much lower because the narrowband ArF radiation is produced by selective amplification of a small region of the ArF emission spectrum. The reduction in precision is enough that the required measurement duration must be increased by several orders of magnitude. As illustrated by the subsequent example, this makes the rotational measurement technique impractical for most engineering applications.

Other Error Sources

Following error sources were also quantified in our study: beam path absorption between the observation window and the measurement location, temperature variation across the measurement volume, and flow rate effects at the measurement location. Analytical models and experimental observations indicate that error sources account for less than 1-K error for beam path distances of 3–4 cm over the temperature and pressure ranges of interest (300–550 K, 1–6 atm). Therefore, for the experimental conditions of interest, the significant uncertainty and error sources are quantum noise, nonlinear process errors (O_2^+ fluorescence and saturation), collisional quenching, and vibrational relaxation.

Practical Considerations for Aerodynamic Measurements

Provided that the vibrational relaxation error is negligible, the remaining error and uncertainty sources need to be balanced to obtain the desired accuracy. In general, the laser fluence is limited by the nonlinear process errors. The number of shots can then be chosen to reduce the quantum noise uncertainty to an acceptable level. Collisional quenching error will not be affected by experimental conditions. Measurement volume will be chosen to satisfy the desired spatial resolution, and collection solid angle and collection efficiency will be maximized within the limits of available equipment.

The error balancing process may be illustrated using an example. Consider a gas temperature measurement where a 3-K accuracy is desired, that is, 99% of the measured values must fall within ± 1.5 K of the true temperature. The approximate temperature is 400 K, and the flow pressure is 2.0 ± 0.2 atm ($P_{O_2} = 0.4 \pm 0.004$ atm). The measurement volume is 0.01 mm^3. The collection solid angle is 0.1 sr, and the collection efficiency is 0.01 (same as the reference values for Fig. 5).

First, the allowed accuracy is budgeted equally between error and uncertainty sources as shown in Fig. 10. From Fig. 7, the pressure-dependent error due to collisional quenching is calculated as ± 0.26 K (1.3 K/atm $\times$ 0.2 atm). The allowable error due to nonlinear sources is then 0.49 K. Figure 6 indicates that the laser fluence must be limited to 20 J/cm^2 to achieve this accuracy.

For normal error distribution, 99% of the readings fall below the mean value plus 2.33σ. The desired σ is then 0.32 K (0.75 K/2.33), and σ^{ref} may be read from Fig. 5 as 3.07 K. The number of shots needed to achieve the desired uncertainty limit can then be calculated using Eq. (3) as follows:

$$N = \left(\frac{\sigma_T^{\text{ref}}}{\sigma_T}\right)^2 \left(\frac{E^{\text{ref}}}{E}\right)\left(\frac{P_{O_2}^{\text{ref}}}{P_{O_2}}\right)\left(\frac{V^{\text{ref}}}{V}\right)\left(\frac{\Omega^{\text{ref}}}{\Omega}\right)\left(\frac{\eta_c^{\text{ref}}}{\eta_c}\right) N^{\text{ref}}$$

$$= \left(\frac{3.07\text{ K}}{0.32\text{ K}}\right)^2 \left(\frac{10\text{ J/cm}^2}{20\text{ J/cm}^2}\right)\left(\frac{1\text{ atm}}{0.4\text{ atm}}\right)\left(\frac{1\text{ mm}^3}{0.01\text{ mm}^3}\right)$$

$$\times \left(\frac{0.1\text{ sr}}{0.1\text{ sr}}\right)\left(\frac{0.01}{0.01}\right) \times 1\text{ shot} \approx 12{,}000\text{ shots} \qquad (6)$$

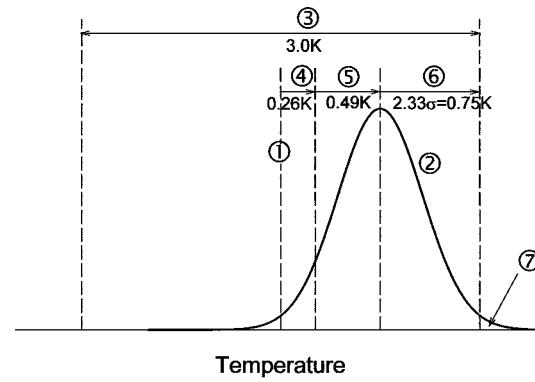

Fig. 10 To determine optimum measurement conditions, the allowable temperature inaccuracy (3) is budgeted between collisional quenching error (4), nonlinear process error (5), and quantum noise (6); only 1% of the temperature readings have greater than 1.5 K temperature error (7). Here (1) is the true temperature and (2) is the probability distribution of the temperature measurements.

In general, the optical temperature measurement technique is about 2000 times slower than corresponding optical velocity measurement techniques such as LDA and PIV. The optical temperature measurement technique is limited by quantum noise uncertainty and nonlinear process errors. The velocity measurement technique, on the other hand, is limited by seeding and data acquision. At the typical ArF laser frequency of 100 Hz, it would require 2 min to make a 12,000-shot measurement at a given point. If an automated positioning system is used, 1000 point measurements (corresponding to a 10^3 grid) can be taken in 33.3 h. By comparison, the laser Doppler anemometry system at NASA John H. Glenn Research Center at Lewis Field makes velocity measurements at 1000 points in less than 1 min.

Conclusions

The objective of this study is to quantify experimentally the error and uncertainty sources for the oxygen LIF gas temperature measurement technique. The information presented in this study may be used to determine experimental conditions for gas temperature measurements.

The optimum data reduction scheme is spectral normalization. This scheme accounts for the dependence of oxygen LIF signals on extraneous parameters such as laser fluence, measurement volume, collection solid angle, and gas pressure. Spectral normalization divides the oxygen LIF spectrum between 200 and 270 nm into temperature-sensitive and temperature-insensitive signals. The ratio of the total signals in the two region types is then used as the temperature diagnostic.

The dominant uncertainty source is quantum noise originating from the discrete nature of light. The dominant error source is nonlinear process errors for low-speed flows. However, collisional quenching may also be significant for flows where the pressure is unknown or variable.

For high-speed measurements above 300 K, the dominant error source is the slow vibrational relaxation time of oxygen molecules. The spatial resolution requirement must be large compared to the distance covered by the flow over the vibrational relaxation period.

The optimum experimental conditions are chosen by dividing the allowable temperature inaccuracy between the error and uncertainty sources. In general, nonlinear process errors will limit the laser fluence. The number of shots per measurement will then be determined by the remaining uncertainty allowance.

Acknowledgment

This study was sponsored by NASA John H. Glenn Research Center at Lewis Field, with Anthony J. Strazisar as Technical Monitor.

References

[1]Massey, G. A., and Lemon, C. J., "Feasibility of Measuring Temperature and Density Fluctuations in Air Using Laser-Induced O_2 Fluorescence," *IEEE Journal of Quantum Electronics*, Vol. QE20, No. 5, 1984, pp. 454–457.

[2]Lee, M. P., and Hanson, R. K., "Calculations of O_2 Absorption and Fluorescence at Elevated Temperatures for A Broadband Argon–Fluoride Laser Source at 193 nm," *Journal of Quantitative Spectroscopy and Radiative Transfer*, Vol. 36, No. 5, 1986, pp. 425–440.

[3]Laufer, G., McKenzie, R. L., and Huo, W. M., "Radiative Processes in Air Excited by an ArF Laser," *Optics Letters*, Vol. 13, No. 2, 1988, pp. 99–101.

[4]Miles, R. B., Connors, J. J., Howard, P. J., Markovitz, E. C., and Roth, G. J., "Proposed Single-Pulse Two-Dimensional Temperature and Density Measurements of Oxygen and Air," *Optics Letters*, Vol. 13, No. 3, 1988, pp. 195–197.

[5]Smith, M. S., Price, L. L., and Williams, W. D., "Laser-Induced Fluorescence Diagnostics Using a Two-Line Excitation Method," *AIAA Journal*, Vol. 31, No. 3, 1993, pp. 478–482.

[6]Lee, M. P., Paul, P. H., and Hanson, R. K., "Laser-Fluorescence Imaging of O_2 in Combustion Flows Using an ArF Laser," *Optics Letters*, Vol. 11, No. 1, 1986, pp. 7–9.

[7]Cohen, L. M., Lee, M. P., Paul, P. H., and Hanson, R. K., "Two-Dimensional Imaging Measurements in Supersonic Flows Using Laser-Induced Fluorescence of Oxygen," AIAA Paper 87-1527, 1987.

[8]Laufer, G., McKenzie, R. L., and Fletcher, D. G., "Method for Measuring Temperatures and Densities in Hypersonic Wind Tunnel Air Flows Using Laser-Induced O_2 Fluorescence," *Applied Optics*, Vol. 29, No. 33, 1990, pp. 4873–4883.

[9]Ishida, T., Niimi, T., Fujimoto, T., and Nakayama, H., "Visualization of Supersonic Flow Using O_2-LIPF," *JSME International Journal*, Ser. B, Vol. 39, No. 3, 1996, pp. 533–539.

[10]Ceyhan, I., "A Quantitative Study of the Feasibility of Oxygen Laser Induced Fluorescence for Engineering Gas Temperature Measurements," Ph.D. Dissertation, Dept. of Mechanical Engineering, Massachusetts Inst. of Technology, Cambridge, MA, Feb. 1997.

[11]Coldwell, R. L., and Bamford, G. J., *The Theory and Operation of Spectral Analysis Using ROBFIT*, American Inst. of Physics, New York, 1991, p. 9.

[12]Marcuse, D., *Principles of Quantum Electronics*, Academic Press, New York, 1980, pp. 232–239.

[13]Bevington, P. R., and Robinson, D. K., *Data Reduction and Error Analysis for the Physical Sciences*, 2nd ed., McGraw–Hill, New York, 1992, p. 28.

[14]Cann, M. W. P., Shin, J. B., and Nicholls, R. W., "Oxygen Absorption in the Spectral Range 180–300 nm for Temperatures to 3000 K and Pressures to 50 atm.," *Canadian Journal of Physics*, Vol. 62, 1984, pp. 1738–1751.

[15]Billing, G. D., and Kolesnick, R. E., "Vibrational Relaxation of Oxygen. State to State Rate Constants," *Chemical Physics Letters*, Vol. 200, No. 4, 1992, pp. 382–386.

[16]Powell, J. A., Strazisar, A. J., and Seasholtz, R. G., "Efficient Laser Anemometer for Intra-Rotor Flow Mapping in Turbomachinery," *Journal of Engineering for Power*, Vol. 103, April 1981, pp. 424–429.

R. P. Lucht
Associate Editor